Journal of Alloys and Compounds 509 (2011) 7368–7372

Contents lists available at ScienceDirect

Journal of Alloys and Compounds

journal homepage: www.elsevier.com/locate/jallcom

Influence of silver addition on the microstructure and mechanical properties of squeeze cast Mg–6Al–1Sn–0.3Mn–0.3Ti

Şehzat Açıkgöz, Hüseyin Şevik, S.Can Kurnaz*

Sakarya University, Faculty of Engineering, Department of Metallurgical and Materials Engineering, Adapazarı 54187,Turkey

ARTICLE INFO

Article history:
Received 18 March 2011
Received in revised form 17 April 2011
Accepted 20 April 2011
Available online 27 April 2011

Keywords:
Mg–6Al alloy
Silver
Microstructure
Mechanical properties

ABSTRACT

In this study, the effect of silver (0, 0.2, 0.5, and 1 wt.%) on the microstructure and mechanical properties of a magnesium-based alloy (Mg–Al 6 wt.%–Sn 1 wt.%–Mn 0.3 wt.%–Ti 0.3 wt.%) were investigated. The alloys were produced under a controlled atmosphere by a squeeze-casting process. X-ray diffractometry revealed that the main phases are α-Mg, α-Ti, β-$Mg_{17}Al_{12}$ and Al_8Mn_5 in the all of alloys. In addition to, $Al_{81}Mn_{19}$ phase was found with Ag additive. Besides, the amount of β-$Mg_{17}Al_{12}$ phase was decreased with increasing the amount of Ag. The strength of the base alloy was increased by solid solution mechanism and decreasing the amount of β-$Mg_{17}Al_{12}$ phase with addition of Ag. Furthermore, existence of $Al_{81}Mn_{19}$ phase can be acted an important role in the increase on the mechanical properties of the alloys.

© 2011 Elsevier B.V. All rights reserved.

1. Introduction

In order to reduce of both CO_2 emission and the fuel cost of transport, the structural applications of magnesium alloys in the automotive industry are pioneered because of their low density and high specific strength. However, the extensive usage of magnesium alloys is limited for their relatively low strength and room temperature ductility than that of aluminum alloys. Therefore, main requirement imposed on magnesium alloys is high strength and ductility [1–5]. Among the commercial magnesium alloys, magnesium–aluminum based alloys such as AM60 and AM50 are endowed with a good combination of cast ability and ductility. Nevertheless, it is well known that Al containing Mg alloys include the β-$Mg_{17}Al_{12}$ compound that deleteriously influences the mechanical properties such as tensile strength and impact resistance. The third alloying element such as strontium (Sr), calcium (Ca), tin (Sn), silver (Ag) and rare earth elements is essential for improving the mechanical properties by removing the detrimental effect of the β-$Mg_{17}Al_{12}$ compound in magnesium–aluminum based alloys[4–15]. Silver with rare earth elements is the most effective alloying element for such proposes which result in significant improvement. However, the high cost of these alloys compared with conventional magnesium alloys has limited their applications [13–15]. Sn and Ti are relatively inexpensive alloying elements. It is well known that Sn alloying element can improve the mechanical properties of magnesium–aluminum alloys through its solubility. Ti has pronounced the grain-refining on the Mg–Al alloys even low concentration and can improve the mechanical properties [7,9,16–19]. Hence, in this study, initially, 1 wt.% Sn and 0.3 wt.% Ti alloy elements are added to Mg–Al alloy instead of rare earth elements and the effect of Ag on the microstructure and mechanical properties of the alloy are investigated.

2. Experimental details

The alloys with compositions listed in Table 1 were prepared in a stainless steel crucible with an electric resistance furnace protected by CO_2-0.2% SF_6 from commercially pure magnesium, aluminum, tin and silver. Manganese and titanium were added using Al–10Mn and Al–6Ti master alloys. The casting parameters were as follows: the melt was held at 760 °C casting temperature for 10 min., and stirred to ensure the homogeneity in a mold at 270 °C under 100 MPa.

Metallographic samples were cut firstly on a wire erosion machine. Grinding was performed using silicon carbide (SiC) grinding papers up to 1200 grit. Prior to polishing, the samples were rinsed with ethanol, and then polishing was performed with a 0.05 μm alumina suspension. The specimens for optical microscopy (OM) were chemically etched in acetic picric (5 ml acetic acid, 6 g picric acid, 10 ml distilled water, 100 ml ethanol). In addition, the distribution of alloying elements in the structure was verified by using a scanning electron microscopy (SEM) instrument (JEOL 6060LV) with an energy-dispersive spectrometer (EDS). X-ray diffraction (XRD) analysis was also carried out to identify the

* Corresponding author. Tel.: +90 2642955789; fax: +90 2642955549.
E-mail address: ckurnaz@sakarya.edu.tr (S.Can Kurnaz).

0925-8388/$ – see front matter © 2011 Elsevier B.V. All rights reserved.
doi:10.1016/j.jallcom.2011.04.112

Table 1
The chemical composition of the investigated alloys (mass fraction, %).

Alloy no	Alloy	Al	Mn	Sn	Ti	Ag	Mg
Alloy 1	Mg–6Al–1Sn–0.3Mn–0.3Ti	5.941	0.272	0.984	0.303	–	Bal.
Alloy 2	Mg–6Al–1Sn–0.3Mn–0.3Ti–0.2Ag	5.918	0.271	0.989	0.311	0.224	Bal.
Alloy 3	Mg–6Al–1Sn–0.3Mn–0.3Ti–0.5Ag	5.901	0.275	0.987	0.297	0.431	Bal.
Alloy 4	Mg–6Al–1Sn–0.3Mn–0.3Ti–1Ag	5.932	0.261	0.978	0.289	0.942	Bal.

phases present in the experimental alloys using a Rigaku D-Max 1000 X-ray diffractometer with Cu Kα radiation.

Brinell hardness tests of the alloys were carried out on ground and polished samples with a ball diameter of 2.5 mm and an applied load of 31.25 kg. At least 10 impressions were made to determine the mean value of the hardness at different locations to circumvent the effect of any alloying element segregation. Tensile tests were performed using an Instron 3367 universal testing machine with a run velocity of 0.2 mm/s at room temperature. Each test was repeated for ten times, and the average values were accepted as the experimental result. Un-notched impact test samples were cut on a wire erosion machine and test specimens measured 55 mm × 10 mm × 10 mm and then polished. The testing was carried out using a Charpy impact test

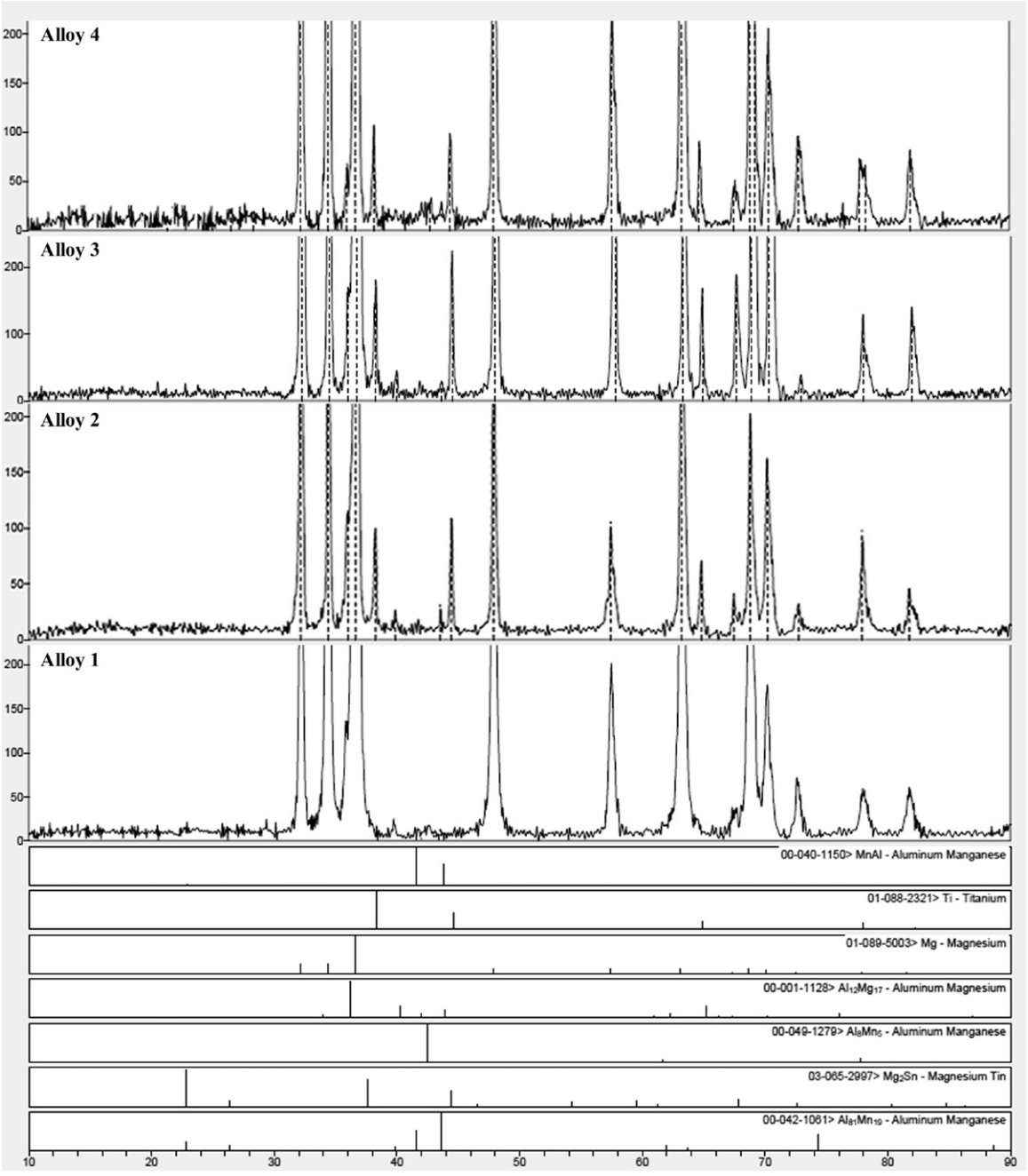

Fig. 1. The XRD spectrums of alloy series.

machine at room temperature and at least three runs were performed.

3. Results and discussion

3.1. Microstructure and characterization

The as-cast alloys were examined by XRD as shown in Fig. 1. The X-ray results revealed that the main components were α-Mg, α-Ti, β-$Mg_{17}Al_{12}$ and Al_8Mn_5 in the all alloys. In addition to main components, $Al_{81}Mn_{19}$ phase was only observed in alloys with silver. It was thought that silver acted effective role for $Al_{81}Mn_{19}$ phase. Besides, the diffraction peak intensity of the β-$Mg_{17}Al_{12}$ phase decreases with the increase of silver content but the diffraction peak intensity of α-Ti increases comparing with base alloy, whereas the intensity of Al_8Mn_5 peak is nearly constant with increasing Ag content. Furthermore, it is not observed any Mg–Sn and Ag based intermetallics in all alloys tested.

Fig. 2 shows the SEM microstructure of the alloys. The microstructure of alloy 1 mainly consists the primary α-Mg dendrite grains with eutectic phases (Al-riched α-Mg + β-$Mg_{17}Al_{12}$) surrounding their boundaries (Fig. 2a). Fig. 2(b) and (c) represents the microstructures of alloy 2 and 4 respectively, indicate that the morphologies of the intermetallic β-$Mg_{17}Al_{12}$ phase in the Ag containing alloys are similar with alloy 1. In addition, the network structure of eutectic α-Mg is changed with increasing Ag content from continuous state to non-continuous.

EDS analysis on the alloy 1 was carried out to define the components as shown in Fig. 3(a). According to the atomic ratio, it could be deduced that the first and second spot in Fig. 3(b) was α-Ti and Al_8Mn_5 phase and third and fourth spot could be decided as α-Mg and β-$Mg_{17}Al_{12}$, respectively. Furthermore, it was proved by EDS of alloy 1 while all Sn was solved both in the primary α-Mg grains and $Mg_{17}Al_{12}$ phase, some of Ti element was found as a metallic form and the rest of Ti dissolved in the aluminum–manganese intermetallic. Fig. 3(b) and (c) shows the microstructures and EDS analysis of the alloys 2 and 4. According to atomic ratio, $Al_{81}Mn_{19}$ intermetallic phase was observed with addition to Ag (Fig. 3(b) spot 1). It is clearly seen that some of Sn and Ti dissolved in the $Al_{81}Mn_{19}$ intermetallic phases. Silver is not found in the aluminum–manganese type compounds. Furthermore, it could be assumed from spots 2, 3 and 4 in Fig. 3(b) that Ag was solved both in the primary α-Mg grains and β-$Mg_{17}Al_{12}$ phase. And also spot 5 was revealed presence of α-Ti. The mapping EDS results supported the above findings about alloy 2. At this time one could observed that Ag element was generally founded in the eutectic areas. Besides, it can be said that from EDS mapping in Fig. 3(c) (alloy 4), the amount of Ag in the β-$Mg_{17}Al_{12}$ phase was increased with increasing Ag additive comparing with alloy 2.

The hardness, yield strength, ultimate tensile strength, elongation and impact strength values of these alloys were listed in Table 2. As can be seen from Table 2, the hardness value of alloy 1 increases with increasing alloying silver concentration. Alloy 4 exhibits the best hardness increment as 16 per cent (from 50HRB to 58HRB) higher than those of the alloy 1. This is probably the result of solid solution hardening due to the solubility of Ag in $Mg_{17}Al_{12}$ and the primary α-Mg. Furthermore, with increasing silver element, α-Ti and $Al_{81}Mn_{19}$ intermetallic phases were occurred at the grain boundaries which could help to improve the hardness of it.

The results of tensile tests reveal that rise of Ag concentration causes an increment in yield and tensile strength while a little bit decreasing the elongation of the alloy 1. The ultimate tensile strength of alloy 1 was improved by 39% (from 190 MPa to 265 MPa) due to the addition of 1 wt.% Ag. Generally, the mechanical

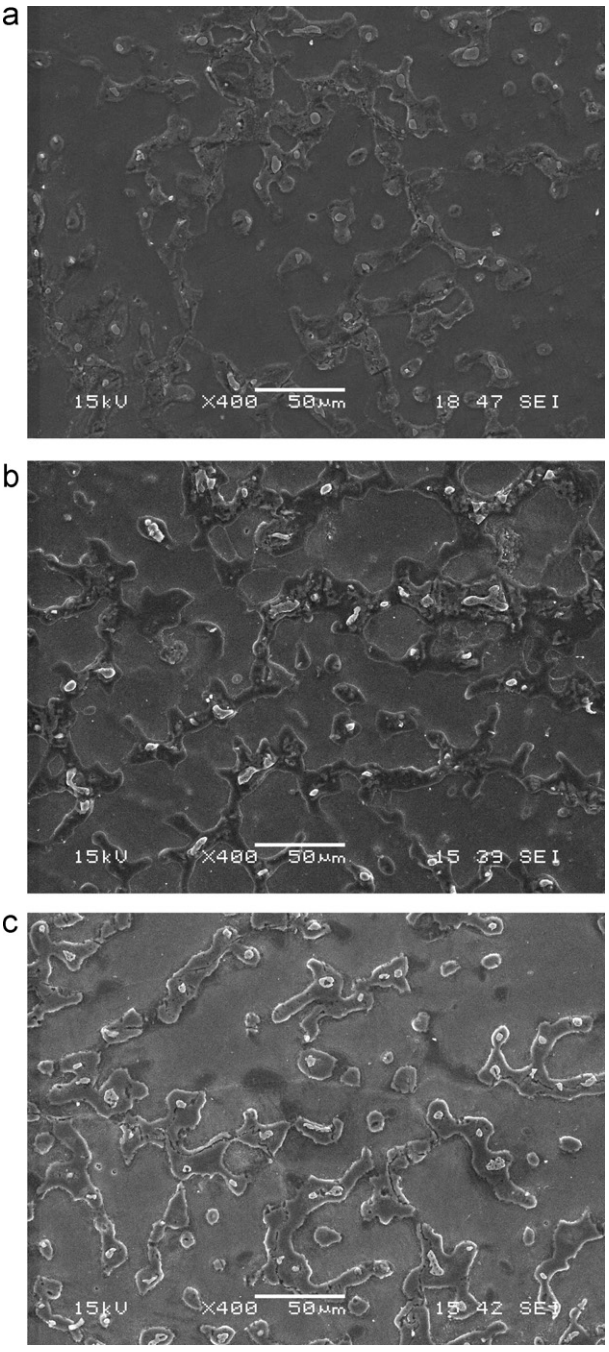

Fig. 2. SEM micrograph showing microstructure of: (a) alloy 1, (b) alloy 2 and (c) alloy 4.

properties of the alloys can improve via solid solution strengthening or/and precipitation strengthening. Besides the size, shape, quantity and distribution of secondary phases can influence the mechanical properties of the alloy [4,8,13,20]. In this study, the improvement of the tensile strength of the alloy 1 mainly comes from the solid solution strengthening of α-Mg, $Mg_{17}Al_{12}$ with silver and existing α-Ti and $Al_{81}Mn_{19}$ intermetallic phases. In addition this effect, as mention earlier in Fig. 2, the continuous form of eutectic area was changed with increasing silver content to non-continuous state. Furthermore, detrimental effect of the β-$Mg_{17}Al_{12}$ phase on the tensile strength reduced with increasing Ag element due to amount of the β-phase decreased. It is believed that the above effects can be effective for high strength. On the other hands, even though little drop was seen on the elongation

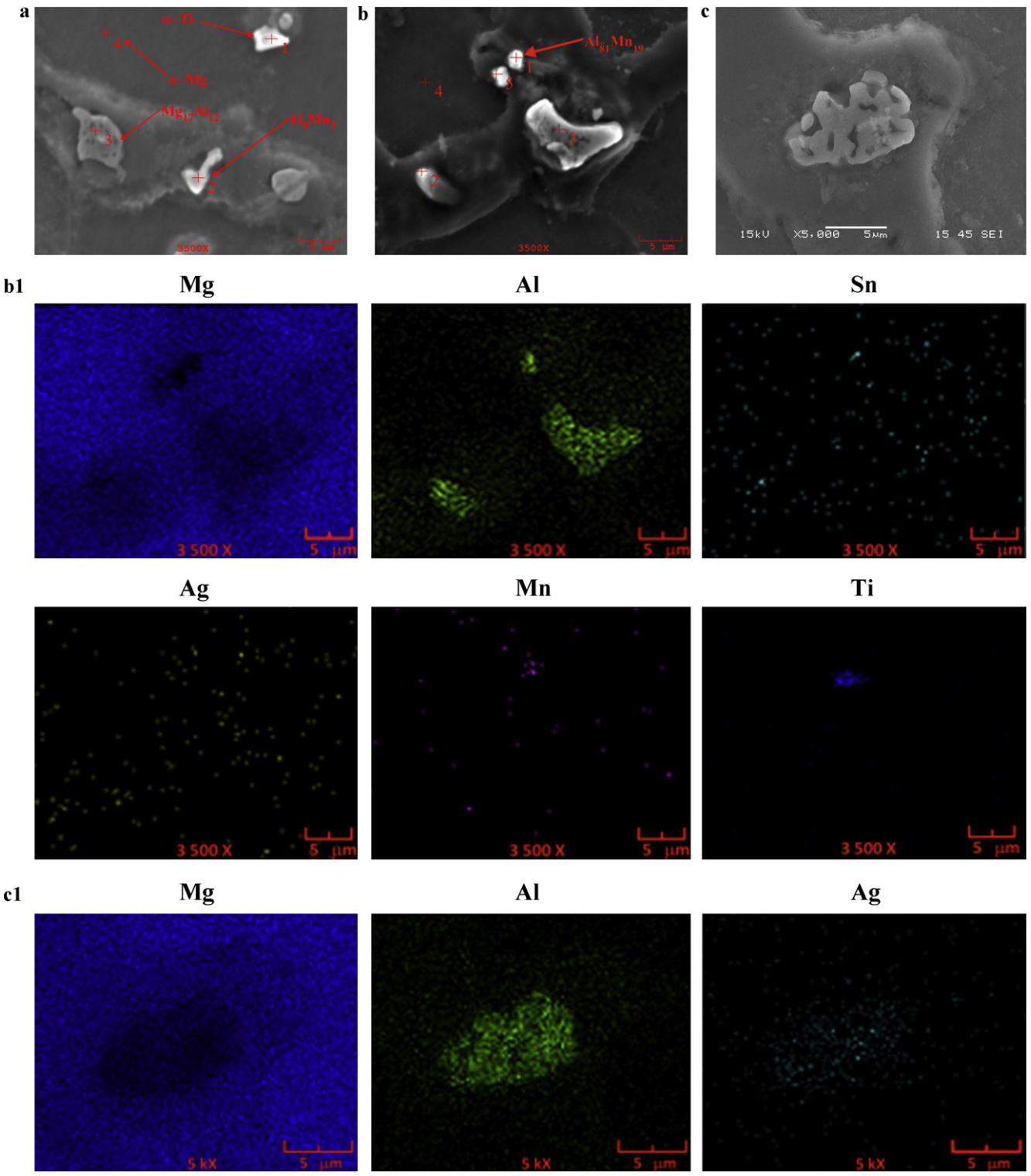

Fig. 3. EDS analysis showing microstructure of: (a) alloy 1, (b) alloy 2 and (c) alloy 4.

Table 2
Hardness, yield strength, ultimate tensile, elongation and impact strength of the tested materials.

	Hardness (HBN)	Yield strength (MPa)	Tensile strength (MPa)	ε (%)	Impact strength (J)
Alloy 1	50 ± 1	115 ± 5	190 ± 3	9.3 ± 0.2	18 ± 0.5
Alloy 2	53 ± 2	118 ± 1	220 ± 5	9.0 ± 0.4	18 ± 0
Alloy 3	56 ± 0	123 ± 6	250 ± 5	9.0 ± 0.3	20 ± 1
Alloy 4	58 ± 1	128 ± 4	265 ± 8	8.8 ± 0.4	23 ± 2

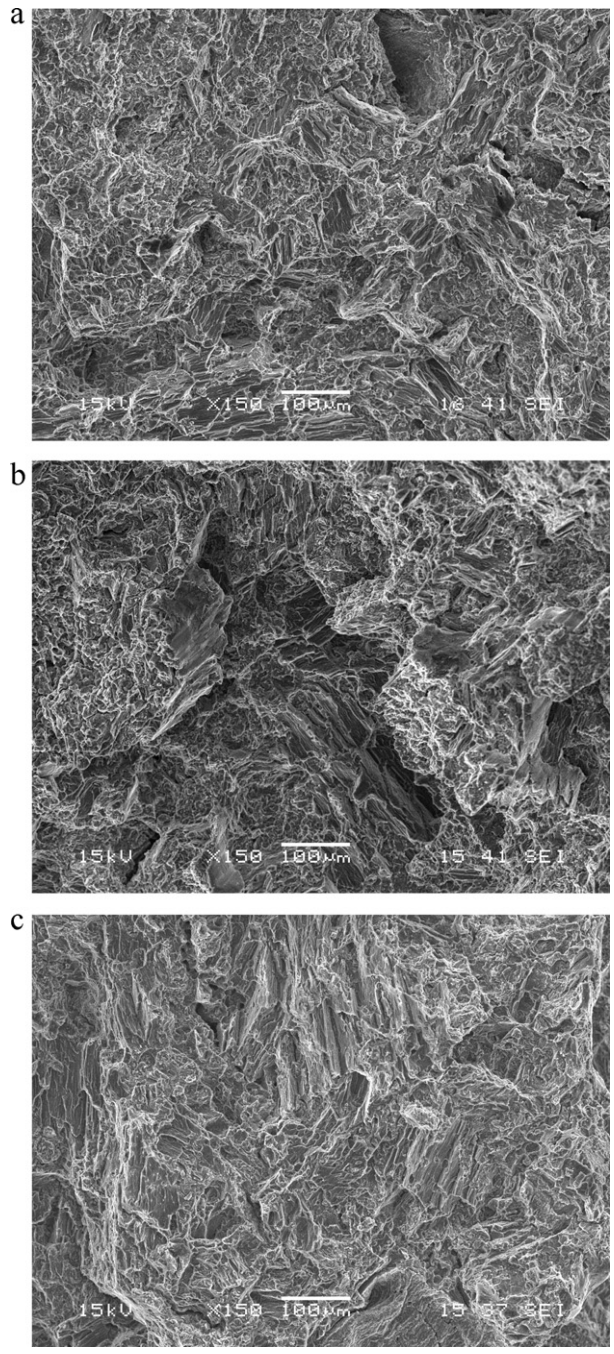

Fig. 4. SEM fractographs showing the morphology of fractured surfaces: (a) Alloy 1, (b) Alloy 2, (c) Alloy 4.

with silver addition, it could be said that the ductility of the alloys was close to each other.

The differences in the fracture surface of tensile specimens via SEM manifests the fracture behavior of the alloys, which is shown in Fig. 4. It can be seen that the observed fracture mode of the alloys is mixed-mode fracture having features associated with dimple rupture and flat facets that may be dealing with brittle fracture of second-phase particles such as β-$Mg_{17}Al_{12}$, α-Ti, $Al_{81}Mn_{19}$. The fracture surface of alloy 1 shows relatively deeper and more amount of dimples than that of alloys containing Ag. On the other hands, brittle fracture features was more dominant in the alloys containing Ag compared with base alloy.

The impact strength value of alloy 1 was found 18J. The result was in accordance with literature. Similar results were reported by Sevik et al. [7]. As can be seen from Table 2, the impact strength of alloy 1 was considerably increased with increasing Ag and improved by 27% (from 18J to 23J) due to the addition of 1 wt.% Ag. The main parameters affecting the impact strength are solid solution hardening due to the solubility of the silver element in the α-Mg, $Mg_{17}Al_{12}$ and the amount of brittle β-$Mg_{17}Al_{12}$ decreased. Besides, existence of the α-Ti and $Al_{81}Mn_{19}$ phase can be acted an important role in the increase on the impact resistance of the alloys.

4. Conclusions

In this present study, influence of addition of Ag on the microstructure and mechanical properties of squeeze cast alloy 1 has been investigated. The following results were obtained:

(1) Metallographic studies and X-ray diffractometry revealed that the main phases are α-Mg, α-Ti, β-$Mg_{17}Al_{12}$ and Al_8Mn_5 in the all alloys. However, with addition of Ag, $Al_{81}Mn_{19}$ phase was found. It is observed that silver dissolved into both α-Mg and β-$Mg_{17}Al_{12}$. Having increased silver element, the amount of Ag in the β-$Mg_{17}Al_{12}$ phase was increased. Furthermore, it can be said that from XRD analysis, the amount of β-$Mg_{17}Al_{12}$ phase was decreased with increasing the Ag alloying element.
(2) Addition of Ag to alloy 1 improved the mechanical properties of the alloy 1. While the hardness, tensile and impact value of alloy 1 increased with increasing alloying element concentration, the elongation decreased little bit.
(3) The fracture surface of alloy 1 shows relatively deeper and more amount of dimples than that of alloys containing Ag. On the other hands, brittle fracture features were more dominant in the alloys containing silver compared with alloy 1.

Acknowledgements

The authors would like to thank the Scientific and Technical Research Council of Turkey-TÜBİTAK for financial support in this research.

References

[1] B.L. Morike, T. Ebert, Mater. Sci. Eng. A 302 (2001) 37–45.
[2] A. Yu, S. Wang, N. Li, H. Hu, J. Mater. Process. Technol. 191 (2007) 247–250.
[3] H. Hu, J. Mater. Sci. 33 (1998) 1579–1589.
[4] D. Schwam, J. Wallace, Y. Zhu, S. Viswanathan, S. Iskander, Enhancements in Magnesium Die Casting Impact Properties, Case Western Reserve University, Ohio, 2000.
[5] M. Zhou, H. Hu, N. Li, J. Lo, J. Mater. Eng. Perform. 14 (2005) 539–545.
[6] A.K. Dahle, Y.C. Lee, M. Nave, P. Schaffer, D. StJohn, J. Light Met. 1 (2001) 61–72.
[7] H. Sevik, S. Açıkgöz, S.C. Kurnaz, J. Alloys Compd. 508 (2010) 110–114.
[8] D.G. Leo Prakash, D. Regener, J. Alloys Compd. 461 (2008) 139–146.
[9] Y.V.R.K. Prasad, K.P. Rao, N. Hort, K.U. Kainer, Mater. Sci. Eng. A 502 (2009) 25–31.
[10] T.A. Leil, N. Hort, W. Dietzel, C. Blawert, Y. Huang, K.U. Kainer, K.P. Rao, Trans. Nonferrous Met. Soc. China 19 (2009) 40–44.
[11] S. Li, B. Tang, D. Zeng, J. Alloys Compd. 437 (2007) 317–332.
[12] G. Barucca, R. Ferragut, D. Lussana, P. Mengucci, F. Moia, G. Riontino, Acta Mater. 57 (2009) 4416–4425.
[13] I. Stloukal, J. Cermak, Comp. Sci. Technol. 68 (2008) 2799–2803.
[14] G.B. Hamu, D. Eliezer, A. Kaya, Y.G. Na, K.S. Shin, Mater. Sci. Eng. A 435–436 (2006) 579–587.
[15] Y.C. Lee, A.K. Dahle, D.H. StJohn, Metall. Mater. Trans. A 31A (2000) 2895–2906.
[16] J. Buha, J. Mater. Sci. 43 (2008) 1220–1227.
[17] P. Zhao, Q. Wang, C. Zhai, Y. Zhu, Mater. Sci. Eng. A 444 (2007) 318–326.
[18] M.X. Liang, W. Xiang, L.X. Lin, Y. Lei, Trans. Nonferrous Met. Soc. China 20 (2010) 397–401.
[19] T.R. Ramachandran, P.K. Sharma, K. Balasubramanian, World Foundry Congress, 2008, pp. 189–193.
[20] N. Hort, Y. Huang, K.U. Kainer, Adv. Eng. Mater. 8 (2006) 235–240.